Structural and morphological characterization of nanosized TiO_2 particles prepared by sol-gel method

C. BANDAS(RATIU)[a,b*], C. LAZAU[b], A. DABICI[c], P. SFARLOAGA[b], N. VASZILCSIN[c], V. TIPONUT[a,c], I. GROZESCU[b]

[a]*National Institute for Research and Development in Microtechnologies, Bucharest, 126A, Erou Iancu Nicolae Street, 077190, Bucharest, Romania*

[b]*National Institute for Research and Development in Electrochemistry and Condensed Matter, Timisoara, Condensed Matter Department, 1 P. Andronescu Street, 300254, Timisoara, Romania*

[c]*"Politehnica"University of Timisoara, 2 Vasile Parvan Bd., 300223, Timisoara, Romania*

Undoped, Ag-doped TiO_2 and N-doped TiO_2 anatase nanocrystals were successfully prepared from titanium tetraisopropoxide by sol-gel method. The as-prepared TiO_2 nanocrystals were structural and morphological characterized by X-ray diffraction, DRUV-VIS spectroscopy, FT-IR spectroscopy, SEM microscopy and EDX analysis. The presence of doping ions, Ag and N, was confirmed by EDX elemental analysis. Also, the results shows that the anatase TiO_2 has a particle size in the nanometer range about 20-30nm, calculated by Scherrer's relation and also confirmed by SEM images.

(Received March 18, 2011; accepted April 11, 2011)

Keywords: Sol-gel, N-doped TiO_2, Ag-doped TiO_2, Nanometer size

1. Introduction

TiO_2 or titania is a very well-known and well-researched material due to the stability of its chemical structure, biocompatibility, physical, optical and electrical properties and also due to their unique properties and potential applications in catalysis [1-3], photo-catalysis [4-8], sensors [9], solar cells [10], energy storage [11], and gene therapy [12]. It exists in three crystalline phases namely anatase, rutile, brookite [13]. Anatase type TiO_2 has a crystalline structure that corresponds to the tetragonal system (with dipyramidal habit) and is used mainly as a photocatalyst under UV irradiation. Rutile type TiO_2 also has a tetragonal structure (with prismatic habit) and is the thermodynamically most stable phase. Brookite phase has an orthorhombic crystalline structure [13]. It is well known that the photocatalytic activity of TiO_2 is related with crystal structure [1]. Also, the surface area, particle size, film thickness and UV light intensity have been seen to be the additional parameters influencing the photocatalytic activity of TiO_2 [1]. On the other hand, the modification of TiO_2 by doping with metallic and nonmetallic ions can also affect the crystallization process, influencing the photocatalytic efficiency of TiO_2.

The advantages derived from TiO_2 and doped TiO_2 as photocatalysts have prompted much research in the field [14]. Various methods are available for the preparation of TiO_2-based photocatalysts, such as electrochemical [15-19], thin films and spin coating [20], precipitation [21, 22], hydrothermal and solvothermal [23-25], chemical solvent and chemical vapour decomposition (CSV & CVD) [26, 27], ultrasonic irradiation [28], two-route sol-gel [14, 29, 30] and sol-gel [31-35]. The benefits derived from preparing TiO_2 by sol-gel method, which include synthesis of nanosized crystallized powder of high purity at low temperature, preparation of composite materials, and production of homogenous materials have driven many researchers to use this method for preparing TiO_2-based photocatalyst.

Sol–gel is one of the most exploited methods; it is used mainly to produce thin film and powder catalysts. Many studies revealed that different variants and modifications of the process have been used to produce pure thin films or powders in large homogeneous concentration and under stoichiometry-control [36, 37].

TiO_2 semiconductor has a high band-gap ($E_g > 3.2$eV), excited only by UV sources with wavelengths shorter than 388 nm in order to inject electrons into the conduction band and to leave holes in the valence band [38]. In the last decade, numerous studies have been recently performed to enhance electron-hole separation and to extend the adsorption range of TiO_2 into visible range. These studies include doping metal/nonmetal ions into the TiO_2 lattice [39], dye photosensitization on the TiO_2 surface [40], and deposition of noble metals [41]. From the doping metal ions, silver is particularly suitable for industrial applications due to its low cost and easy preparation. The effects of Ag dopants on the lattice or surface of TiO_2 have been investigated [38]. He et al. [42] have investigated the effect of Ag doping on the microstructure and photocatalytic activity of TiO_2 films prepared by sol-gel method.

In 2001, Asahi et al. [43] characterized an N-doped TiO_2 film by the reactive sputtering method, and reported that the N-doped film had a high photoefficiency at the visible range.

In this paper, nanosized Ag-doped TiO_2 and N-doped TiO_2 particles were prepared by a simple sol-gel method using titanium tetraisopropoxide like Ti precursor. The physical properties of the prepared particles were investigated by X-ray diffractometer (XRD), Fourier transform infrared spectroscopy (FT-IR), diffuse reflectance UV-VIS spectroscopy (DRUV-VIS), scanning electron microscopy (SEM) and energy dispersive X-ray analysis (EDX).

2. Experimental

Titanium (IV) tetraisopropoxide (TTIP, 98%), silver nitrate ($AgNO_3$), urea, ethanol and ammonia (NH_3) were purchased from ALDRICH Company.

Nanosized Ag-doped TiO_2 and N-doped TiO_2 particles were prepared by a simple sol-gel method.

1. The synthesis method for nanosized undoped TiO_2 and Ag-doped TiO_2 (TiO_2-Ag) materials was reported in our previous paper [44]

2. The N-doped TiO_2 (TiO_2-N) nanocrystals were successfully synthesized by sol-gel method. An amount of ethanol was stirred with 5 mL TTIP and after 10 minutes, 30mL of distilled water was added in dropwise. The pH of the initial solution was 5.5 and before adding the doping precursor (ureea) the pH was adjusted with 1N NH_3 solution until 8. Two different quantities were used for TiO_2 doping, such as 2 wt% (TiO_2-N2) and 3 wt% (TiO_2-N3).

The obtained solutions were filtered, washed and dried to 60ºC for 5 hours. For crystallization the materials were annealed separately into an oven for 2 hours. In case of undoped TiO_2 the annealing temperature was set at 250ºC (TiO_2-250) and 350ºC (TiO_2-350) and for doped TiO_2 nanocrystals at 500ºC (TiO_2-Ag2-500, TiO_2-Ag3-500, TiO_2-N2-500 and TiO_2-N3-500) respective 600ºC (TiO_2-Ag2-600, TiO_2-Ag3-600, TiO_2-N2-600 and TiO_2-N3-600).

The materials were structural and morphological characterized by specific methods. The crystallinity of the prepared samples was measured by X-Ray diffraction (XRD) using PANalytical X'PertPRO MPD Diffractometer with Cu tube. The light absorption properties of the materials were studied by UV-VIS diffuse reflectance spectroscopy (DRUV-VIS) using a Lambda 950 Perkin Elmer device. The bond vibration of modified materials was analyzed by Fourier transform infrared spectrometry (FT-IR) using a JASCO FT/IR-430 spectrometer. A scanning electron microscopy (SEM) using Inspect S PANalytical model coupled with the energy dispersive X-ray analysis detector (EDX) was used to characterize the external surfaces of the nanocrystals, using catalyst powder supported on carbon tape.

3. Results and discussion

Figures 1i and ii presents the *XRD* patterns of undoped TiO_2 (i), TiO_2-Ag2 and TiO_2-Ag3 (ii), TiO_2-N2 and TiO_2-N3 (iii) annealed at different temperatures. It is well known that annealing improved the crystallization of TiO_2 powders and accelerated the transformation from amorphous phase to anatase or rutile phase. The XRD patterns confirms that at low temperature, about 250ºC (Fig. 1i, spectra a), the crystalline phase for undoped TiO_2 reveals pure anatase form (2 theta: 25.3º, 37º, 37.8º, 38.6º, 48º, 54º, 55°[45]). By increasing the temperature at 350ºC (Fig. 1i, spectra b) the anatase phase is almost disappeared and the rutile form (2 theta: 27.3º, 35.9º, 41.1º, 54.1º [46]) is predominantly. This aspect is explained by the effect of annealing temperature on the anatase form, which become metastable at higher temperature and it is converted into stable rutile phase [44].

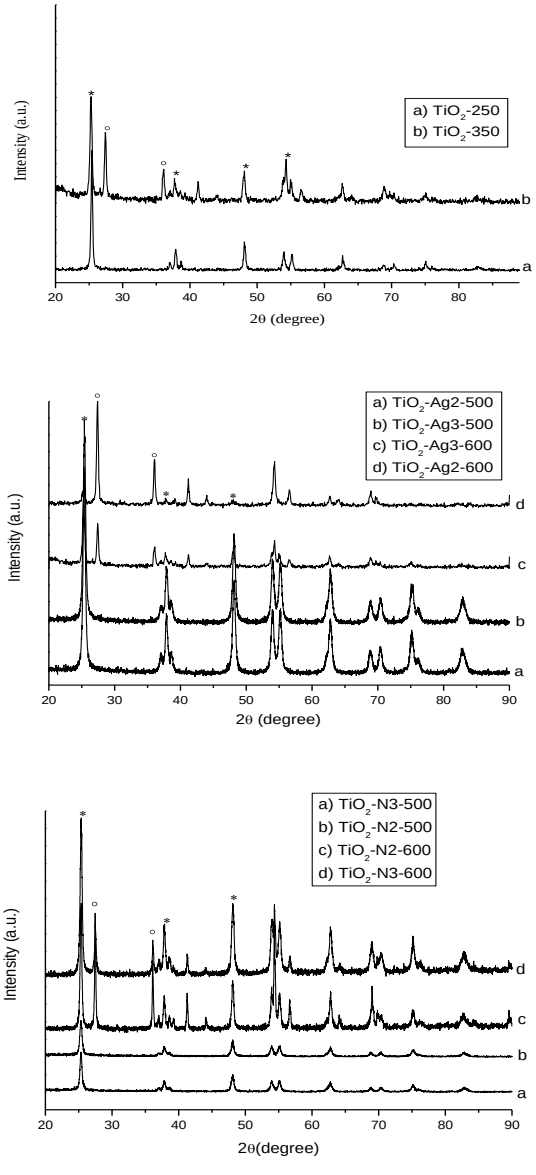

Fig. 1. XRD patterns of i) undoped TiO_2, ii) TiO_2-Ag2 and TiO_2-Ag3, iii) TiO_2-N2 and TiO_2-N3 at different calcinations temperatures (-anatase, ○–rutile)*

The XRD patterns are different when the metallic, respective non-metallic ions are presents. The TiO_2-Ag and TiO_2-N exhibited a different behavior when the calcinations temperature is around 500°C (Fig. 1ii spectra

a and b, Fig. 1iii spectra a and b). For both obtained materials pure anatase crystalline phase is present at 500°C without the appearance of rutile form. The increasing of the temperature around 600°C determined the rutile phase appearance like predominant crystalline phase (Fig. 1ii spectra c and d, Fig. 1iii spectra c and d). The literature data reports that the transformation of the anatase phase into rutile phase around 600ºC and the transformation temperature depends on the precursors type and on the synthesis conditions and properties of the particles [38]. Also, it can be seen that the doping degree and the type of dopants did not influence the phase transition.

Based on the XRD patterns were calculated the particles size of the prepared materials. Crystallite size was calculated by Scherrer's formula i.e. $D=k\lambda/\beta cos\theta$ [47], λ is the wavelength of the X-ray radiation (λ = 0.15406 nm), k is the Scherrer's constant (k=0.89), and β is the line width at the half maximum height. The average particle size obtained for anatase phase from XRD data for undoped, Ag-doped TiO_2 and N-doped TiO_2 nanocrystals were in the range of 20-30nm (Table 1).

Table 1. Average particle sizes by Scherrer's equation.

Material type	***Particle size (nm)***
TiO_2-250	25.4
TiO_2-Ag2-500	23.0
TiO_2-Ag3-500	21.4
TiO_2-N2-500	31.9
TiO_2-N3-500	26.7

The light absorption properties of the prepared materials crystallized in pure anatase phase were studied by DRUV-VIS performed under ambient conditions in the wavelength range of 300-550 nm. Figures 3i and ii presents the *DRUV-VIS* spectra recorded for TiO_2-250, TiO_2-Ag2-500 and TiO_2-Ag3-500 (Fig. 2i), respective TiO_2-250, TiO_2-N2-500 and TiO_2-N3-500 (Fig. 2ii). Spectra analysis shows that undoped TiO_2 synthesized by sol-gel route adsorbs only in UV domain at the wavelength around 390 nm. The literature data presented that the anatase form of undoped TiO_2 has band-gap energy about 3.2eV, which means that for electrons excitation the semiconductor needs to be expose to a radiation with the wavelength smaller or equal with 385 nm, namely in UV domain [48].

For the Ag-doped TiO_2 nanocrystals (TiO_2-Ag2-500 and TiO_2-Ag3-500) it can be seen a slight adsorption movement in the visible domain at the wavelength range 390-450 nm. The doping amount influences the spectra movement in the visible domain (Fig. 2i).

From Fig. 3ii it can be seen that the bands attributed to the stretching modes of Ti-OH bound has different values depending of materials type: TiO_2-250 (Fig. 3ii, curve a) presents a large adsorption band in the range 3382-3490 cm^{-1}, for TiO_2-N3-500 (Fig. 3ii, curve c) it can be seen a movement of the wavenumber range to 3373-3548 cm^{-1} and for TiO_2-N2-500 (Fig. 3ii, curve b) the Ti-OH vibration bands became weakly, the wavenumber range being 3487-3343 cm^{-1}.

At the wavenumber of 1383 cm^{-1} it can be seen a new band attributed to the inflexion vibration of C-H bound. The specific band for inflexion vibrations of water molecules is in the range of 1620-1645 cm^{-1} [50]. The adsorption from the region 400-600 cm^{-1} reflects the presence of Ti-O-Ti bound (Figs. 3i and ii) [51].

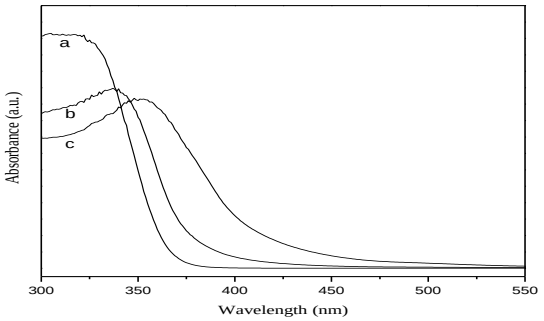

i)

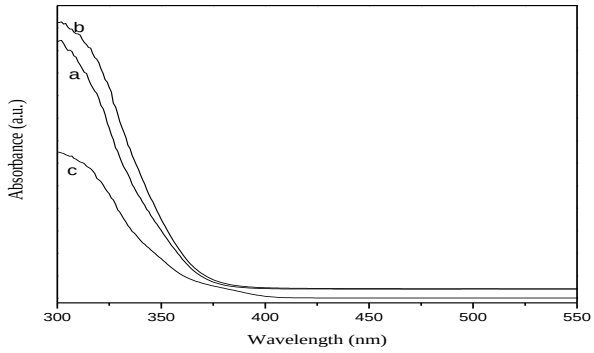

ii)

Fig. 2. DRUV-VIS spectra for i) TiO_2-250 (curve a), TiO_2-Ag2-500 (curve b) and TiO_2-Ag3-500 (curve c) and ii) TiO_2-250 (curve c), TiO_2-N2-500 (curve a) and TiO_2-N3-500 (curve b) obtained by sol – gel method.

For the N-doped TiO_2 nanocrystals (TiO_2-N2-500 and TiO_2-N3-500) the spectra are slightly moved towards wavelength of 400 nm, and when the doping degree is smaller the adsorption band in under 400 nm (Fig. 2ii).
Figures 3i and ii represent the *FT-IR* spectra of TiO_2-250, TiO_2-Ag2-500 and TiO_2-Ag3-500 (Fig. 3i), respective TiO_2-250, TiO_2-N2-500 and TiO_2-N3-500 (Fig. 3ii). A large adsorption band around 3382-3490 cm^{-1} attributed to the stretching modes of OH group, indicated the presence of water molecules (Fig. 3i) [49]. Also the presence of bands at the wavenumbers of 2846 cm^{-1} and 2915 cm^{-1} are associated to the symmetric and anti-symmetric stretching modes of C-H bound.

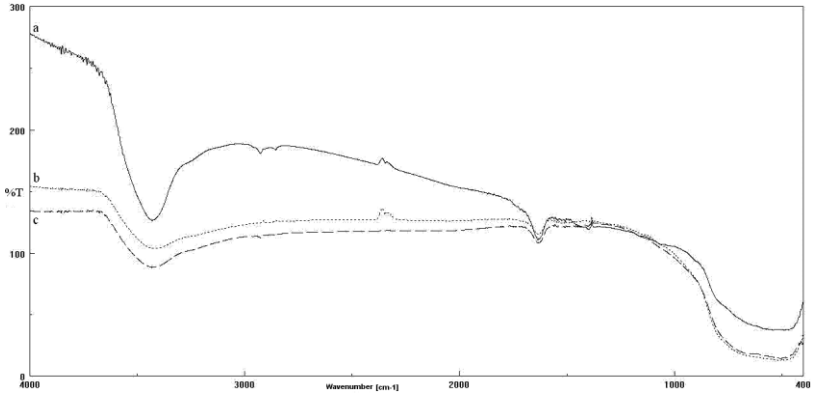

i)

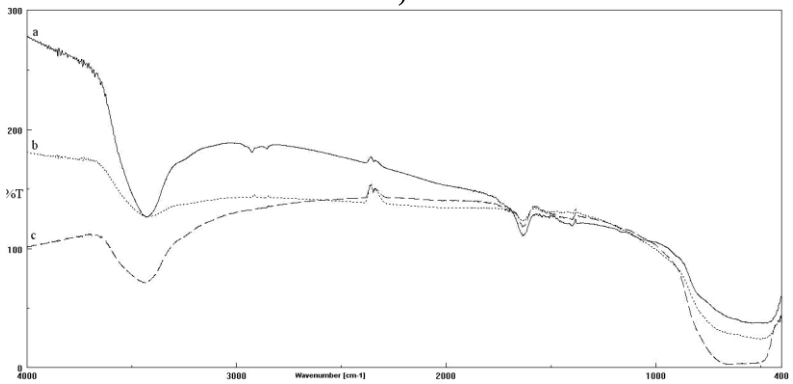

ii)

Fig. 3. FT-IR spectra for (i) TiO_2-250 (curve a), TiO_2-Ag2-500 (curve b) and TiO_2-Ag3-500 (curve c) and (ii) TiO_2-250 (curve a), TiO_2-N2-500 (curve b) and TiO_2-N3-500 (curve c)

For the morphological and structural characterization the obtained materials were characterized by SEM morphology and EDX analysis (Figs. 4-6). Thus are presented examples of SEM images and EDX spectra for undoped TiO_2, Ag-doped TiO_2 and N-doped TiO_2. SEM images evidenced for all the obtained materials the spherical form of TiO_2 nanocrystals, specific for anatase phase [52] highly agglomerated in asymmetric conglomerates (Figs. 4a, 5a, 6a). At a higher magnification (mag. 200.000x), it is obvious that the anatase TiO_2 (spherical form) has particle size in the nanometer range. EDX microprobe provided a semiquantitative elemental analysis of the surface indicating the materials purity. Thus, for undoped TiO_2 (Fig. 4b) EDX spectra evidenced the Ti and O presence, for Ag-doped TiO_2 and N-doped TiO_2 its shows the Ag (Fig. 5b) respective N (Fig. 6b) ions presence. Also, the doping degree did not influence the size, shape or agglomeration degree of the particles.

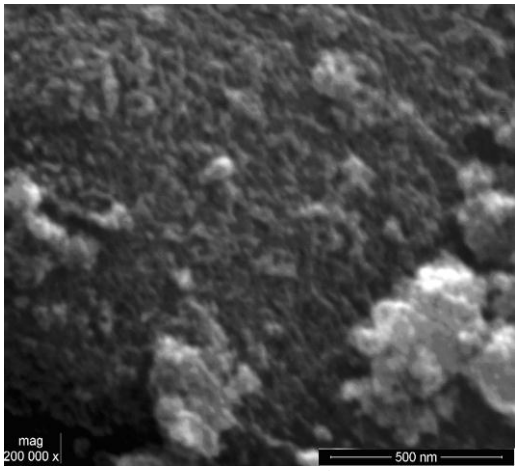

a)

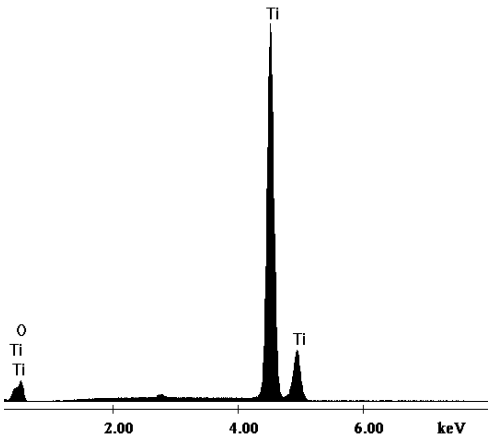

b)

Fig. 4. a) SEM morphology and b) EDX analysis for TiO_2-250 synthesized by sol-gel method

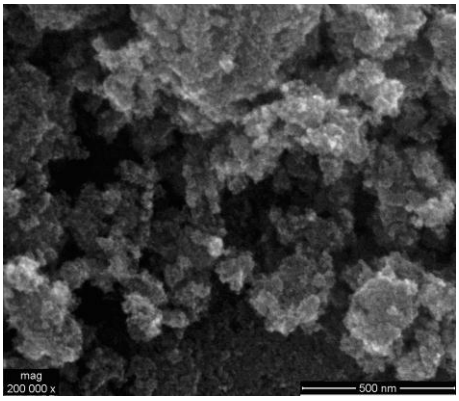

a)

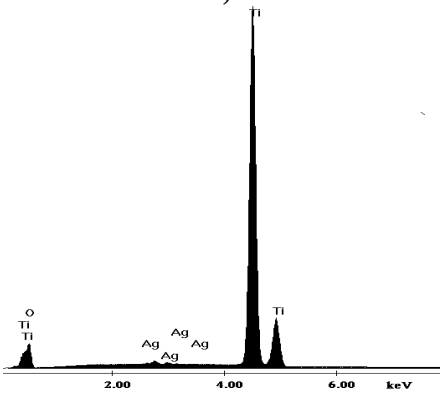

b)

Fig. 5. a) SEM morphology and b) EDX analysis for TiO_2-Ag3-500 synthesized by sol-gel method

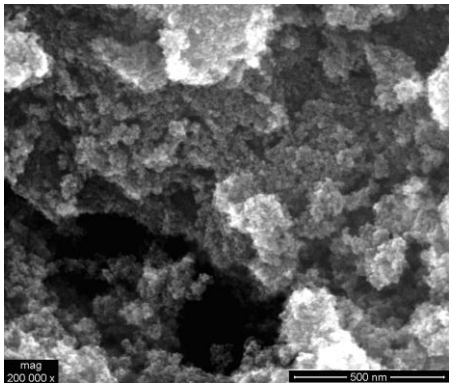

a)

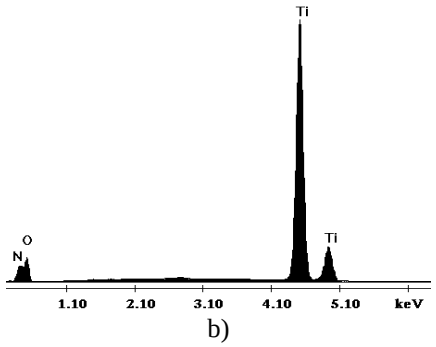

b)

Fig. 6. a) SEM morphology and b) EDX analysis for TiO_2-N3-500 synthesized by sol-gel method

4. Conclusions

Undoped, Ag-doped TiO_2 and N-doped TiO_2 nanocrystals were successfully obtained by sol-gel method using titanium tetraisopropoxide like Ti precursor. It was used two doping degree, namely 2wt% and 3wt%. Based on XRD patterns the optimum annealing temperature was set up at 250°C for undoped TiO_2 and 500°C for doped TiO_2 nanocrystals in order to obtain pure anatase phase. The average particle size obtained for anatase form calculated by Scherrer's equation was in the nanometer range, 20-30 nm. SEM images presented the spherical form of TiO_2 nanocrystals, specific for anatase phase and also confirmed the nanometer particle size. EDX analysis confirmed the materials purity and presence of doping ions (Ag and N).

Acknowledgements

The research presented in this paper is supported by the *Sectoral Operational Programme Human Resources Development (SOP HRD)* financed from the European Social Fund and by the Romanian Government under the contract number *POSDRU/81/1.5/S/63700.* This experiment was also supported by the Romanian National Project 72-156 NANOZEOREZID, Romanian Ministry of Education and Research.

References

[1] J. Garcia-Serrano, E. Gomez-Hernandez, M. Ocampo-Fernandez, U. Pal, Current Applied Physics **9**, 1097 (2009).
[2] P. Forzatti, Catal. Today 62, 51 (2000).
[3] Z. Ma, Y. Yue, X. Deng, Z. Gao, J. Mol. Catal. A **178**, 97 (2002).
[4] C. A. Linkous, G.J. Carter, D.B. Locuson, A. J. Ouellette, D.K. Slattery, L.A. Smitha, Environ. Sci. Technol. **34**, 4754 (2000).
[5] J.K. Yang, A.P. Davis, Environ. Sci. Technol. **34**, 3796 (2000).
[6] A. Maldoti, A. Molinari, R. Amadeni, Chem. Rev. **102**, 3811 (2002).
[7] M. Anpo, M. Takeuchi, J. Catal. **216**, 505 (2003).
[8] A. Fujishima, T.N. Rao, D.A. Tryk, J. Photochem. Photobiol. C: Photochem. Rev. **1**, 1 (2000).
[9] I. Hayakawa, Y. Iwamoto, K. Kikuta, S. Hirano, Sens. Actuators, B: Chem. **62**, 55 (2000).
[10] M. Adachi, J. Am. Chem. Soc. **126**, 14943 (2004).
[11] S. Zhang, L.M. Peng, Q. Chen, G.H. Du, G. Dawson, W.Z. Zhou, Phys. Rev. Lett. **91**, 256103 (2003).
[12] T. Paunesku, T. Rajh, G. Wiederrecht, J. Master, S. Vogt, N. Stojicevic, M. Protic, B. Lai, J. Oryhon, M. Thurnauer, G. Woloschak, Nat. Mater. **2**, 343 (2003).
[13] G. Li Puma, A. Bono, D. Krishnaiah, J.G. Collin, J. Hazard. Mater. **157**, 209 (2008).
[14] U.G. Akpan, B.H. Hameed, Appl. Catal. A: Gen. **375**, 1 (2010).

[15] W. Song, W. Xiaohong, Q. Wei, J. Zhaohua, Electrochim. Acta **53**, 1883 (2007).
[16] X.H. Wu, Z.H. Jiang, H.L. Liu, X.D. Li, X.G. Hu, Mater. Chem. Phys. **80**, 39 (2003).
[17] S. Karuppuchamy, N. Suzuki, S. Ito, T. Endo, Curr. Appl. Phys. **9**(1), 243 (2009).
[18] L. Fan, N. Ichikuni, S. Shimazu, T. Uematsu, Appl. Catal. A: Gen. **246**, 87 (2003).
[19] J. Chen, J. Zhang, Y. Xian, X. Ying, M. Liu, L. Jin, Water Res. **39**. 1340 (2005).
[20] K. R. Patil, S.D. Sathaye, Y.B. Khollam, S.B. Deshpande, N.R. Pawaskar, A.B. Mandale, Mater. Lett. **57**, 1775 (2003).
[21] Y. Li, G.P. Demopoulos, Hydrometallurgy **90**, 26 (2008).
[22] J. Sun, L. Qiao, S. Sun, G. Wang, J. Hazard. Mater. **155**, 312 (2008).
[23] W. Zhiyu, C. Haifeng, T. Peisong, M. Weiping, Z. Fuan, Q. Guodong, F. Xianping, Colloids Surf. A: Physicochem. Eng. Aspects **289**, 207 (2006).
[24] F. Wang, Z. Shi, F. Gong, J. Jiu, M. Adachi, Chin. J. Chem. Eng. **15**(5), 754 (2007).
[25] F. Peng, L. Cai, L. Huang, H. Yu, H. Wang, J. Phys. Chem. Solids **69** (7), 1657 (2008).
[26] T.K. Ghorai, D. Dhak, S.K. Biswas, S. Dalai, P. Pramanik, J. Mol. Catal. A: Chem. **273**, 224 (2007).
[27] X. Zhang, L. Lei, Mater. Lett. **62**, 895 (2008).
[28] F. Peng, L. Cai, H. Yu, H. Wang, J. Yang, J. Solid State Chem. 181, 130 (2008).
[29] M. Huang, C. Xu, Z. Wu, Y. Huang, J. Lin, J. Wu, Dyes Pigments **77**, 327 (2008).
[30] F.B. Li, X.Z. Li, Chemosphere **48**, 1103 (2002).
[31] X. Fan, X. Chen, S. Zhu, Z. Li, T. Yu, J. Ye, Z. Zou, J. Mol. Catal. A: Chem. **284**, 155 (2008).
[32] A. Zaleska, J.W. Sobczak, E. Grabowska, J. Hupka, Appl. Catal. B: Environ. **78**, 92 (2008).
[33] D.-G. Huang, S.-J. Liao, J.-M. Liu, Z. Dang, L. Petrik, J. Photochem. Photobiol. A: Chem. **184**, 282 (2006).
[34] J.-W. Shi, J.-T. Zheng, Y. Hu, Y.-C. Zhao, Mater. Chem. Phys. **106**, 247 (2007).
[35] G. Liu, X. Zhang, Y. Xu, X. Niu, L. Zheng, X. Ding, Chemosphere **59**, 1367 (2005).
[36] S. Bu, Z. Jin, X. Liu, T. Yin, Z. Cheng, J. Mater. Sci. **41**(7), 2067 (2006).
[37] R. Campostrini, M. Ischia, L. Palmisano, J. Therm. Anal. Calorim. **71** (3), 997 (2003).
[38] M. S. Lee, S.-S. Hongb, M. Mohseni, J. Molec. Catal. A: Chem. **242**, 135 (2005).
[39] S.D. Mo, L.B. Lin, J. Phys. Chem. Solids **55**, 1309 (1994).
[40] K. Vinodgopal, D.E. Wynkoop, P.V. Kamat, Environ. Sci. Technol. **30**, 1660 (1996).
[41] V. Vamathevan, R. Amal, D. Beydoun, G. Low, S. McEvoy, J. Photochem. Photobiol. A **148**, 233 (2002).
[42] C. He, Y. Yu, X.F. Hu, A. Larbot, Appl. Surf. Sci. **200**, 239 (2002).
[43] R. Asahi, T. Mohikawa, T. Ohwaki, K. Aoki, Y.Taga, Science **293**, 269 (2001).
[44] P. Sfirloaga, S. Novaconi, C. Lazau, C. Ratiu, C. Orha, I. Grozescu, N. Vaszilcsin, J. Optoelectron. Adv. Mater. **12** (9), 1884 (2010).
[45] A. N. Okte, E. Sayinsoz, Sep. Purif. Technol. **62** 535, (2008).
[46] B. Qi, L. Wu, Y. Zhang, Q. Zeng, J. Zhi, J. Colloid Interface Sci. **345**, 181 (2010).
[47] C. Lazau, P. Sfirloaga, C. Orha, C. Ratiu, I. Grozescu, Mater. Lett. **65**, 337 (2011).
[48] J. Zhu, W. Zheng, B. He, J. Zhang, M. Anpo, J. Mol. Catal. A: Chem. **216**, 35 (2004).
[49] W.-C. Hung, S.-H. Fu, J.-J. Tseng, H. Chu T.-H. Ko, Chemosphere **66**, 2142 (2007).
[50] Y.-F. Chena, C.-Y. Lee, M.-Y.Yenga, H.-T. Chiua, J. Crystal Growth **247**, 363 (2003).
[51] T. Yamauchi, R. Barillon, E. Balanzat, T. Asuka, K. Izumi, T. Masutani, K. Odaa, Radiation Measurements **40**, 224 (2005).
[52] F. Cot, A. Larbot, G. Nabias, L. Cot, J. Eur. Ceram. Soc. **18**, 2175 (1998).

*Corresponding author. cornelia_ratiu@icmct.uvt.ro